ELSEVIER

Journal of Photochemistry and Photobiology A: Chemistry 147 (2002) 93–101

Journal of Photochemistry and Photobiology A:Chemistry

www.elsevier.com/locate/jphotochem

Nonlinear dependence of solvent polarity effects on twisted intramolecular charge-transfer states and linear relation for electronic spectra in a stilbazolium-like dye

Chuan-Lang Zhan [a,*], Duo-Yuan Wang [b]

[a] *Organic Solids Laboratory, Center for Molecular Science, Institute of Chemistry, Chinese Academy of Sciences, Beijing 100080, PR China*
[b] *Laboratory of Photochemistry, Center for Molecular Science, Institute of Chemistry, Chinese Academy of Sciences, Beijing 100080, PR China*

Received 11 June 2001; received in revised form 20 August 2001; accepted 31 October 2001

Abstract

The photophysical properties of a stilbazolium-like dye, *trans*-1-(*N*-methylpyrrol-2-yl)-2-(*N*-methyl-4-pyridinium)-ethene iodide, in 20 solvents and its photochemistry were investigated. A division into two groups in the linear relation between the solvatochromic shifts (absorption, fluorescence emission and corresponding Stokes shifts) and solvent polarity parameter E_T^N was observed. The dipole moments of fluorescence emission and twisted intramolecular charge-transfer state were estimated. The quantum yields of fluorescence and *trans* → *cis* photoisomerization change by almost two orders of magnitude. The rate constant of radiative decay is in the order of 10^7–10^8 s^{-1}, which is about one or two orders of magnitude less than that of the photochemistry decay, whereas the rate constant of the radiationless decay is in the order of 10^8–10^{10} s^{-1}. The nonlinear dependence and division into two groups which differs very much from that in the above linear relation were also observed for the solvent polarity influences on the properties of the twisted intramolecular charge-transfer state. The decay scheme from the excited singlet state was assigned as controlled by the equilibrium constant for interconversion between the twisted and planar conformations, which differs from that of reported organic molecules, such as ordinary stilbazolium dyes, stilbene derivatives, or rhodamine B, etc.

Keywords: Photophysics; Twisted intramolecular charge-transfer state; Stilbazolium-like dye

1. Introduction

The very strong temperature, solvent polarity and viscosity dependence on the photophysical properties of stilbazolium dyes [1–5], which can be used as fluorescence indicators in neurons [6,7], have been usually discussed by invoking single-bond twisting in the excited state towards a "twisted intramolecular charge-transfer (TICT) state" [8,9] (called I* state [3,5] hereafter) as the main decay process of the excited state. As the I* state, whose dipole moment is usually larger than that of the fluorescence emission state (called E* state [3,5] hereafter), is lower in energy than the E* state and the double-bond twisted excited state, e.g., P* state [3,5], so, in general, it acts as the lowest excited state [3,5].

In general, a scheme for the decay kinetic model of stilbazolium dyes can be given as Scheme 1 shows, where molecules are excited by a light $h\nu$ to get the Franck–Condon (F–C) state, followed by relaxation to E* state, from which they can decay to the ground state by fluorescence emission (k_f) or undergo a horizontal reaction to (i) the I* state with rate constant k_1 or (ii) the P* state with rate constant k_P. The molecules at the I* state can undergo either internal conversion to the ground state (I) with rate constant k_{IC} or conversion back to E* state with rate constant k_2. The rate constant of the internal conversion decay k_I from the E* to I* to I states, and then to ground state S_0 can be given by the following:

$$k_I = \frac{k_{IC}k_1}{k_{IC} + k_2} \quad (1)$$

Because there is an interconversion process between the twisted and planar conformations [9–12], so if $k_{IC} \gg k_2$, the present decay rate constant k_I, which exhibits a very strong solvent viscosity dependence, is controlled by the rate constant k_1, e.g., for stilbazolium dyes such as *trans*-1-(4-di-*n*-butylaminobenzyl)-2-(4-*n*-butylsulfonate-pyridinium)-ethene [3]. While as a reverse case, if $k_{IC} \ll k_2$, the rate constant k_I, which does exhibit the solvent viscosity

* Corresponding author. Tel.: +86-10-62639355; fax: +86-10-62559373.
E-mail address: dqzhang@infoc3.icas.ac.cn (C.-L. Zhan).

1010-6030/02/$ – see front matter
PII: S1010-6030(01)00634-7

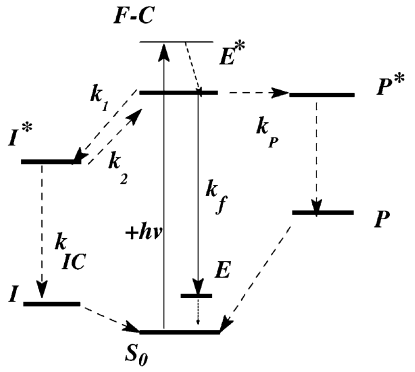

Scheme 1. A reaction scheme of singlet state for a typical stilbazolium dye.

independence, is controlled by the equilibrium constant for interconversion between the twisted and planar conformations, e.g., for rhodamine B [12].

The solvent polarity parameter E_T^N [13] or $E_T(30)$ [13,14] scales, [1] which were derived from the spectral shift of pyridinium *N*-phenolate betaine [14] (called standard dye hereafter) (see below), was usually used for describing the overall solvent polarity influences on the photophysical properties of organic molecules [10,15–19], although Fromherz et al. use the concept of the Born free energy [20,21] to estimate the change of equilibrated solvation energy up to the transition state, based on an assumption that the solvation shell follows the diffusion along the reaction coordinate [3,22].

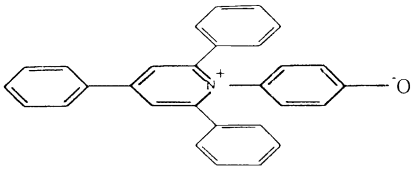

In this paper, we will use the E_T^N-scale to describe the photophysical properties of a stilbazolium-like dye: *trans*-1-(*N*-methylpyrrol-2-yl)-2-(*N*-methyl-4-pyridinium)-ethene iodide (called compound **1** hereafter) (see below), which was first reported for the application in the field of optoelectronics [23].

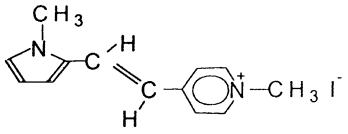

The solvent influences on the photophysical properties, in particular, on the properties of the I* state of compound **1** have been investigated in detail.

[1] The values of E_T^N are calculated from $E_T(30)$ values which are the transition energies from the ground to F–C states of the standard dye solutions in different solvents through the relation $E_T^N = [E_T(30)^{Sol} - E_T(30)^{TMS}]/(E_T(30)^{water} - E_T(30)^{TMS})$ with $E_T(30) = hcN_A\nu_a = 2.859\times10^{-3}\nu_a^{sol}(cm^{-1}) = 28591/\lambda^a(nm)$, here TMS is tetramethylsilane, N_A is Avogadro constant (e.g., see, [13]).

2. Experimental section

2.1. Materials and solvents

Trans-isomer of compound **1** was synthesized and purified as follows. In a mixture of ethanol and water (with a volume ratio of 1:1), sodium hydroxide (Beijing Chemical Factory of China) was used as a catalyst for the condensation of 4,*N*-dimethyl-pyridinium iodide [24] and *N*-methyl pyrrole-2-carbonaldehyde (Fluka). The melting point of the crystalline-product after recrystallizing from the mixture of ethanol and water was 256.2–256.3 °C. The product was identified by its ^{1}H-NMR spectrum and elemental analysis [25]. 9,10-Diphenylanthracence (EGA) and rhodamine B (Beijing Chao-Yang Xi-Hui Hua-Gong Chang of China) were used as received.

All of the analytical grade solvents used in this work were purchased from Beijing Chemical Factory of China, and distilled before use on the pertinent inorganic salts to collect the middle fractions [26]. Deionized water was used.

2.2. Apparatus and procedures

The corrected emission spectra were recorded on a Hitachi 850 fluorescence spectrophotometer. Quantum yields of fluorescence ϕ_f were determined on a Hitachi F-4500 fluorescence spectrophotometer with rhodamine B ($\phi_f^{REF} = 0.5$) [27] in high purified nitrogen-saturated ethanol at 25 °C as standard and the same absorbance at $\lambda_{exc} = 450$ nm, typically 0.1–0.5. A correction of ϕ_f for the refractive index of the solvents did not seem necessary in view of the magnitude of this effect relative to that of the change in solvent polarity. In nonpolar solvents where *trans* → *cis* photoisomerization could contribute, the samples were irradiated for the shortest periods possible (the conversion is less than 10%). The quantum yields of fluorescence were determined as a function of temperature from 25 to 80 °C if possible. Corrections were made for the temperature dependence of the extinction coefficient. The effect of oxygen on ϕ_f (less than 10%) was negligible, so the air-saturated solutions of the sample were used. The estimated errors were all below 10% for the quantum yields of fluorescence.

The quenching of the quantum yield of fluorescence was performed as follows. To a 10^{-6} M solution of compound **1** in acetonitrile, small volumes of a 10^{-3} M solution of 9,10-diphenylanthracence in acetonitrile were added.

The lifetimes τ_f were measured on a HORIBA NAES-1100 time-resolved fluorescence spectrophotometer with a response width of 200 ps. The excitation light with a wavelength at $\lambda = 450$ nm was obtained by a monochromatic slice from a high-pressure hydrogen lamp with emission wavelengths in the UV–Vis region. The fluorescence was detected at about 520 nm achieved also by a monochromatic slice. The measured decay curves can be reasonably well fitted by the iterative deconvolution method using a

single-exponential model. The estimated errors were all below 15% for the lifetime.

The absorption spectra of solutions of the *trans*-isomer were measured similarly on a Hitachi 557 UV–Vis spectrophotometer. For measurements of quantum yields of the *trans* → *cis* photoisomerization (ϕ_{TC}), a 117 W iodine–tungsten lamp was used with a emission wavelength ranging from 400 to 650 nm which almost coincides with the absorption band of compound **1**. The quantum flux was measured by using 4-nitro-4′-(*N*,*N*-dimethylamino)stilbene in high purified nitrogen-saturated cyclohexane (ϕ_{TC} = 0.28, the position of the photostationary state is 70% for *cis*-isomer) [18]. All of the solutions (typical concentration 10^{-5} M) were air-saturated, and the procedure for determination of the values of ϕ_{TC} was the same as described elsewhere [3]. Because only the *trans*-isomer was used, the extinction coefficients for the *cis*-isomer ε_C were measured by using the Fischer method [28]. The errors of ϕ_{TC} were estimated below ±20%.

3. Calculations

The standard AM1 method (Austin model 1, Hamilton of the MOPAC6.0 program [29]) was used for the calculations of the ground and excited state dipole moments, the bond length, the angles, the twist angles between the planes of the donor or acceptor rings and the ethenyl group, and the charge distribution in the excited state. The keywords of GEO-OK, CHARGE = 1, DIPOLE, PRECISE, CI = (8, 6), SINGLET, EXCITED were used. Note that the keyword of CI = (8, 6) was selected by considering six occupied π-type molecular orbits (MOs) for 12 π-electrons and two unoccupied MOs in a molecule of compound **1**. GEO-OK was used to override interatomic distance check.

4. Results and discussion

4.1. Fluorescence and absorption spectra

The UV–Vis absorption, fluorescence excitation and emission spectra for compound **1** in dimethyl sulfoxide (DMSO) at room temperature are shown in Fig. 1. We can see that the fluorescence excitation and the absorption spectra coincide nearly. Similar results are found in the other solvents. Fig. 2 shows plots of the solvatochromic shifts (absorption, fluorescence emission maxima and corresponding Stokes shifts) versus E_T^N (Table 1) in 20 solvents, from which we can see that all of the experimental points are divided into two groups and may be fitted to form two nearly parallel lines. Their linear regression data are listed in Table 2. The solvents in group *i*-1 are of n- or π-types solvents with *i* represents the absorption (1), fluorescence emission (2) and corresponding Stokes shift (3). The rest of solvents belonging to group *i*-2 are of alkane chlorides

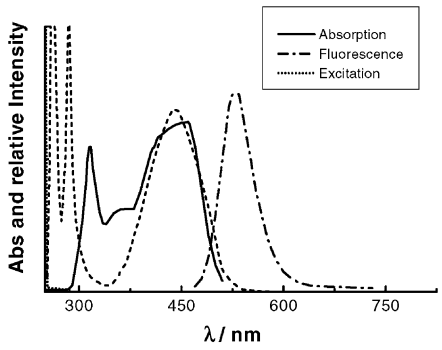

Fig. 1. Absorption (—), fluorescence excitation (···) and corresponding emission spectra (–·–) in DMSO.

and protic solvents. Obviously, the fluorescence emission is lightly dependent of the solvent polarity while the absorption and Stokes shifts do largely. The bluest-shift in chloroform at λ = 518 nm (19 305 cm^{-1}), and the reddest in DMSO and acetonitrile with λ = 526 nm (19 011 cm^{-1}) are observed. In other words, the fluorescence emission is slightly red-shifted with increasing solvent polarity, indicating that the dipole moment of E* state is very small.

The above results suggest that a similar Jablonski diagram depicted in Fig. 3 adequately describes the events which

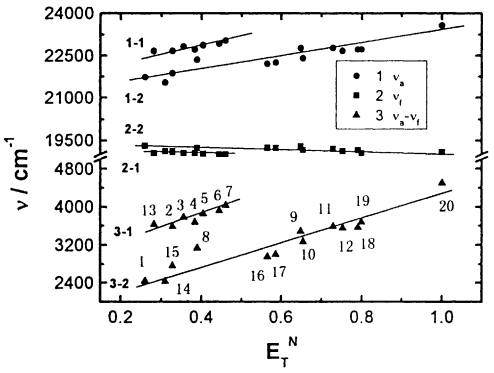

Fig. 2. Plots of linear relationships between the solvatochromic shifts and the solvent polarity parameter E_T^N. The signals 1-1 and 1-2 represent two groups for absorption, 2-1 and 2-2 are two groups for fluorescence, 3-1 and 3-2 are two groups for the corresponding Stokes shifts, respectively. The number codes of the solvents are given in Table 1.

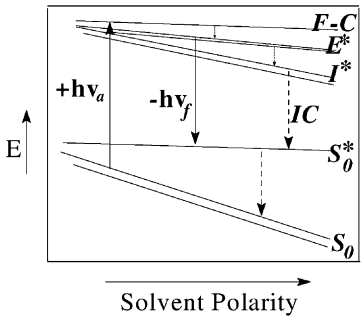

Fig. 3. Energy level diagram for intramolecular charge-transfer states of compound **1**.

Table 1
Solvent polarity parameters, solvent viscosity η, fluorescence quantum yields ϕ_f, the rate constant of radiationless decay k_{nr}, Arrhenius energies E_V (kJ/mol), Arrhenius intercepts, and free energy gap between E* and I* states ΔG^0_{EI} (kJ/mol)[a]

Number	Solvent	E_T^N	BK	Δf	η	ϕ_f	k_{nr} (ns^{-1})	E_V (kJ/mol)	$\ln A_0$	ΔG^0_{EI} (kJ/mol)	$\ln A_{corr}$
1	Chloroform	0.259	0.378	0.565	0.542	0.00005	13.15	7.6	26.2	11.7	26.3
2	2-Butanone	0.309	0.624	0.73	0.378	0.0022	5.68	9.7	26.3	12.1	26.3
3	Acetone	0.355	0.796	0.868	0.303	0.0029	4.29	11.8	26.9	13.6	26.9
4	Butanenitrile	0.383	0.778	0.865	0.567	0.0035	3.55	12.0	25.8	13.3	25.8
5	DMF	0.404	0.836	0.922	0.802	0.0043	2.91	10.9	26.1	11.9	26.1
6	DMSO	0.444	0.844	0.941	1.991	0.0054	2.31	12.6	26.6	13.2	26.6
7	Acetonitrile	0.460	0.863	0.924	0.345	0.0046	2.71	11.6	26.4	11.9	26.4
8	1-Butanol	0.586	0.751	0.768	2.571	0.0043	2.91	12.5	26.7	12.5	26.6
9	Acetic acid	0.648	0.496	0.632	1.131	0.0046	2.71	13.1	26.9	13.5	26.9
10	Ethanol	0.654	0.819	0.892	1.678	0.004	3.12	12.1	26.7	12.7	26.7
11	Formic acid	0.728	0.886	0.950	1.966	0.003	4.17	–	–	–	–
12	Methanol	0.752	0.850	0.910	0.547	0.0027	4.60	12.0	26.6	14.5	26.7
13	Cyclohexanone	0.281	0.738	0.852	2.109	0.0056	2.22	12.6	26.5	14.6	26.4
14	Dichloromethane	0.327	0.596	0.759	0.422	0.007	1.78	10.7	25.5	12.7	25.5
15	1,2-Dichloroethane	0.327	0.767	0.854	0.805	0.0074	1.68	12.4	26.2	13.7	26.1
16	T-Butylalcohol	0.389	0.689	0.793	4.438	0.011	1.12	14.0	26.2	14.9	26.2
17	I-Amylalcohol	0.565	0.739	0.739	3.738	0.017	0.72	14.7	26.3	14.6	26.3
18	Ethyleneglycol	0.790	0.838	0.880	16.79	0.0087	1.43	14.2	26.7	15.4	26.7
19	Formamide	0.799	0.893	0.973	3.302	0.007	1.78	14.7	27.3	16.1	27.8
20	Water	1.000	0.917	0.963	0.89	0.0026	4.84	11.7	26.9	16.7	26.9

[a] The relative error of the quantum yield is about 10%. The rate k_{nr} of radiationless decay are obtained as $k_{nr} = k_I + k_P = k_f^{AV}(\phi_f^{-1} - 1)$ with $k_f^{AV} = 0.0125\,ns^{-1}$. Apparent Arrhenius energy E_V and preexponential factor A_0 describe the temperature-dependent quantum yield of fluorescence as $k_f^{AV}(\phi_f^{-1} - 1) = A_0 \exp(-E_V/RT)$. The values of the viscosity are from [3,13].

Table 2
Solvatochromic intercepts $m_{1\text{-}j}$ (in the unit of cm^{-1}/E_T^N), slopes $n_{2\text{-}j}$ (in the unit of cm^{-1}/E_T^N), the relative linear coefficients R^2, and the dipole moments μ (D) for compound **1** (the Onsager parameter a_w is taken as 6.4 Å)[a]

	ν_a			ν_f			$\nu_a - \nu_f$		
	$m_{i\text{-}ja}$	$n_{i\text{-}ja}$	R^2	$m_{i\text{-}jf}$	$n_{i\text{-}jf}$	R^2	$m_{i\text{-}js}$	$n_{i\text{-}js}$	R^2
$E_T^N(i\text{-}1)$	22076 ± 162	1973 ± 422	0.902	19243 ± 63	-507 ± 170	−0.748	2915 ± 495	2292 ± 495	0.900
$E_T^N(i\text{-}2)$	21106 ± 168	2224 ± 263	0.931	19394 ± 55	-319 ± 81	−0.794	1828 ± 162	2384 ± 254	0.943
μ(D)	–	9.2	–	–	1.5	–	–	7.8	–

[a] i represents absorption (1), fluorescence emission (2) and corresponding Stokes shifts (3) and j represents groups 1 and 2 for each of solvatochromic shifts.

occur upon photoexcitation of compound **1**. In which the S_0^* state represents the E and I states shown in Scheme 1. The lines labeled by S_0, E*, and I* represent the S_0, E* and I* states both in group i-1 (upper line) and in group i-2 solvents (lower line), respectively. The transition energy from the S_0 to F–C states linearly increase, while the emission energy linearly decreases with increasing E_T^N. Based on such analysis, we can rationally assume that the energy difference ΔE_{10} of the I* and I states shown in Scheme 1 linearly decreases with increasing E_T^N, and can be also fitted to form two nearly parallel lines described by Eq. (2) with a positive κ-value (Fig. 3).

$$\Delta E_{10} = \Delta E_{10}^0 - \kappa E_T^N \quad (2)$$

Here, ΔE_{10}^0 is an intercept, representing the energy gap between I* and I states in a certain solvent with $E_T^N = 0$. κ is a slope.

In order to take into account the polarization effects on the E* state, a plot of the Stokes shifts ($\nu_a - \nu_f$) versus another solvent polarity parameter BK (Table 1) according to Eq. (3) yields an intercept $m_S = 1330\,cm^{-1}$, and a slope $n_S = 2799\,cm^{-1}$/BK with a linear correlation coefficient of $R^2 = 0.740$.

$$\nu_a^{sol} - \nu_f^{sol} = (\nu_a^{gas} - \nu_f^{gas}) + \left[\frac{|\mu_e - \mu_g|^2}{hca_w^3}\right] BK \quad (3)$$

Here, BK is defined by $BK = [L(\varepsilon_r) - L(n^2)]/[(1 - L(\varepsilon_r))(1 - L(n^2)^2)]$, where $L(\varepsilon_r)$ and $L(n^2)$ are defined by $L(x) = 2(x-1)/(2x+1)$ with $x = \varepsilon_r, n^2$, where ε_r and n are the bulk static relative permittivity and refractive index of the solvent, respectively [30], and ν is the wavenumber of absorption maximum of the electronic transition of the solute in solution (sol), in gas phase (gas), in absorption (a)

and in fluorescence (f), respectively, μ_g and μ_e are the dipole moments of the ground and excited states, respectively, h the Planck constant, and c the speed of light in vacuum.

As Rettig and co-workers [19] suggested, it is obtained that there are similar values of slopes for the correlation of Stokes shifts against E_T^N and BK values. This means that we could calculate the difference of the ground and excited states dipole moments, as $\Delta\mu_{eg} = 7.8\,D$ by using the average of $n_{3\text{-}1s}$ and $n_{3\text{-}2s}$ with the Onsager radius $a_w = (11.8 \times 6.7 \times 3.4)^{1/3} = 6.4$ angstrom, where 11.8 angstrom is the molecular length, 6.7 angstrom the width (from the two opposite hydrogen of the pyridinio groups), and 3.4 angstrom the thickness (the van der Waals π-cloud of the pyridinio group) [19], because a much higher linear correlation coefficient between Stokes shifts and E_T^N is found.

$$\nu_f^{sol} = \text{constant} - \left(\frac{2}{hca_w^3}\right) \times \left[\frac{(\mu_e - \mu_g)\mu_e(\varepsilon_r - 1)}{\varepsilon_r + 2} - \frac{1}{2}\frac{(\mu_e - \mu_g)^2(n^2 - 1)}{n^2 + 2}\right] \quad (4)$$

Based on Eq. (4) [31] which is usually used to correlate the relation between the fluorescence wavenumber ν_f of the stilbene derivatives [32,33] and solvent polarity, a linear plot (not shown) of ν_f versus another solvent polarity parameter $\Delta f = (\varepsilon_r - 1)/(\varepsilon_r + 2)$ (Table 1) also yields two lines with intercepts $m_I = 19\,447$ and $m_{II} = 19\,591\,cm^{-1}$, slopes $n_I = 449$ and $n_{II} = 483\,cm^{-1}/\Delta f$, and linear correlation coefficients $R_I^2 = 0.880$ and $R_{II}^2 = 0.914$, respectively. We can also see that there are similar values of intercepts and slopes for the correlations of ν_f against both E_T^N and Δf, meaning that the value of μ_e can be calculated using the values of $n_{2\text{-}1f}$ and $n_{2\text{-}2f}$, but because there is a better linear relationship between ν_f and Δf, so the value of μ_e is estimated as 1.5 D by using the average of n_I and n_{II}. Note that the term $0.5(n^2 - 1)/(n^2 + 2) \approx 0.12$ is approximately constant for the solvents employed.

The summary of data calculated using MOPAC program is shown in Table 3. The sum of $\mu_e = 1.5\,D$ and $\Delta\mu_{eg} = 7.8\,D$ yields a ground-state dipole moment $\mu_g = 9.3\,D$ which is very close to a calculated value ($\mu_g = 8.3\,D$). Another the dipole moment of the excited state is obtained as 4.6 D from the calculation using MOPAC program, which is assigned as the dipole moments of twisted excited state, implied by the twist angles of $\theta_1 = 17.1°$ (between the donor and the ethenyl planes labeled by 5-6-7-8 shown in Table 3), and $\theta_2 = -12.3°$ (between the acceptor and the ethenyl planes labeled by 7-8-9-10 shown in Table 3). Note that the negative sign of θ_2 indicates that the direction of θ_2 is opposite to that of θ_1. Therefore, the value of 1.5 D is assigned as the dipole moment of the E* state. The twist angles are calculated as $\theta_1 = -0.04°$ and $\theta_2 = 1.34°$ for the molecules in ground state.

Table 3
Summary of data from calculations using MOPAC program[a]

	The ground state	The I* state
μ (D)	8.3	4.6
θ_1 (°)	−0.04	17.1
θ_2 (°)	1.34	−12.3

[a] θ_1 is the dihedral angle between the planes of pyrrole ring and ethenyl presented by the twist angle of four atoms labeled by 5-6-7-8, and θ_2 is that between ethenyl and pyridinium ring also presented by four atoms labeled by 7-8-9-10. The number codes of atoms are shown in

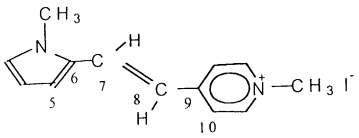

Table 4
The quantum yield of fluorescence ϕ_f, the lifetime τ_f and the rate of radiation k_f in 12 solvents[a]

Solvent	ϕ_f	τ_f (ns)	k_f ($\times 10^7\,s^{-1}$)
Cyclohexanone	0.0056	0.353	1.59
Dichloromethane	0.0070	0.438	1.60
1,2-Dichloroethane	0.0074	0.427	1.73
2-Butanone	0.0022	0.341	0.65
Acetone	0.0029	0.299	0.97
Butanenitrile	0.0035	0.348	1.01
DMF	0.0043	0.355	1.21
DMSO	0.0054	0.330	1.64
Acetonitrile	0.0046	0.281	1.64
Ethanol	0.0040	0.323	1.24
Methanol	0.0027	0.282	0.96
Water	0.0026	0.286	0.91

[a] The relative errors of the quantum yields are all below 10%. The relative errors of the lifetimes are below 15%.

4.2. Quantum yield of fluorescence, lifetime and radiative rate constant

We have measured the quantum yields of the fluorescence ϕ_f and the lifetimes τ_f (Table 4) in 12 solvents. We can see that the values of ϕ_f are in the order of 10^{-3}, and that of τ_f are in the order of 10^2 ps. The radiative rate constants k_f are calculated from ϕ_f and τ_f according to Eq. (5) and listed in Table 4, from which we can see that the values of k_f in 12 solvents range from 0.65 to $1.73 \times 10^7\,s^{-1}$, and change by almost one order of magnitude. The average k_f^{AV} of k_f is $1.25 \times 10^7\,s^{-1}$ and

$$k_f = \frac{\phi_f}{\tau_f} \quad (5)$$

4.3. Photochemistry

We have measured the ratio of the quantum yields of the *trans* → *cis* and *cis* → *trans* photoisomerization ϕ_{TC}/ϕ_{CT} and the quantum yields of the *trans* → *cis* photoisomerization ϕ_{TC} (Table 5) in seven solvents. Then, we calculate ϕ_{CT} from ϕ_{TC} and ϕ_{TC}/ϕ_{CT} in seven solvents (Table 5). We can see that the values of ϕ_{TC} change by almost three orders

Table 5
Molar fraction X_T of the *trans*-isomer of compound **1** in the photostationary state at 25 °C, ratio ϕ_{TC}/ϕ_{CT} of the quantum yields of *trans* → *cis* and *cis* → *trans* photoisomerization from measurements in the photostationary state, individual quantum yields ϕ_{TC} and ϕ_{CT} of *trans* → *cis* and *cis* → *trans* photoisomerization from kinetic data and k_p (see Scheme 1)[a]

Solvents	X_T	ϕ_{TC}/ϕ_{CT}	ϕ_{TC}	ϕ_{CT}	k_P (ns^{-1})
Chloroform	0.52	0.18	0.12	0.67	4.8
Dichloromethane	0.56	0.16	0.10	0.63	0.48
1,2-Dichloroethane	0.76	0.063	0.040	0.63	0.18
Acetone	0.55	0.16	0.10	0.63	1.2
DMSO	0.94	0.012	0.0076	0.63	0.48
Ethyleneglycol	0.85	0.034	0.020	0.59	0.07
Water	0.98	0.0045	0.0027	0.61	0.33

[a] The relative errors are below 20%. The values of ϕ_{CT} are calculated from the ratio ϕ_{TC}/ϕ_{CT} and from ϕ_{TC}. Their errors are around 50%.

of magnitude. The rate constants k_P of the horizontal transition to the P* state are calculated from ϕ_{TC}, ϕ_{CT}, and ϕ_f according to Eq. (6) [3] and are also listed in Table 5, from which we can see that the values of k_P are in the range from 0.07 to 4.8 ns^{-1}, changing by almost three orders of magnitude. The k_P in chloroform and acetone which possess a relatively small viscosity is in the order of ns^{-1} and that in ethylene glycol which bears large viscosity is in the order of 10^{-2} ns^{-1}, showing the viscosity dependence. It must be noted that there could be other factors besides the solvent viscosity influenced on the k_P by taking into account the large difference of the values of k_P in dichloromethane and chloroform whose viscosities are nearly the same:

$$k_P = k_f \left\{ \frac{\phi_{TC}/(1-\phi_{CT})}{\phi_f} \right\} \quad (6)$$

4.4. Intersystem crossing

We have measured the quenching of the relative quantum yield of fluorescence (ϕ_f^0/ϕ_f) by 9,10-diphenylanthracene. The data are shown in Fig. 4. They are described by a Stern–Volmer relation $\phi_f^0/\phi_f = 1 + K_{SV}C_Q$. The quenching constant $K_{SV} = 37\,M^{-1}$ ($R^2 = 0.990$). The Stern–Volmer constants in the order of $10^3\,M^{-1}$ are usual for the quenching of excited singlet states, indicating that the intersystem crossing could be ruled out as an important process of decay from the fluorescence state [3,34].

4.5. Internal conversion decay

We have measured the quantum yields of fluorescence in 20 solvents (Table 1). Each rate constant of radiationless decay k_{nr} including k_P and k_I is calculated from k_f^{AV} and ϕ_f according to Eq. (7) and are listed in Table 1, from which we can see that the values of k_{nr} change by almost two orders of magnitude:

$$k_{nr} = k_I + k_P = k_f^{AV}(\phi_f^{-1} - 1) \quad (7)$$

Because the values of k_P are almost one order of magnitude less than that of k_{nr}, indicating that the solvent dependence of k_P may be negligible compared to that of k_{nr}, so the solvent dependence of k_{nr} can be rationally assumed as controlled mainly by that of k_I. Therefore, we have $k_{nr} \cong k_I$.

A plot of ϕ_f versus E_T^N (not shown) shows that ϕ_f exhibits a strong dependence on the solvent polarity and all solvents are divided into two groups, in which ϕ_f increases initially with increasing E_T^N, then turns over at high E_T^N.

Fig. 5 shows a plot of the logarithm of the rate constants of radiationless decay, $\ln k_{nr}$ (Table 1) against E_T^N, from which we can see that the values of $\ln k_{nr}$ also exhibit a strong dependence on the solvent polarity and all solvents are also divided into two groups labeled by I and II with the same divisions as that in the plot of ϕ_f versus E_T^N. In each group, the values of $\ln k_{nr}$ decrease initially with increasing E_T^N, after getting its minimum in which E_T^N is about 0.56, it then increase. The best fitting these data using Eq. (8) yields an intercept $k_{nr}^0 = 2.17\,(\pm 0.2)\,ns^{-1}$ for group I and $0.88\,(\pm 0.08)\,ns^{-1}$ for group II, with an amplitude $B = 20.0\,(\pm 1.9)$ for group I and $10.1\,(\pm 1.1)$ for group II and a

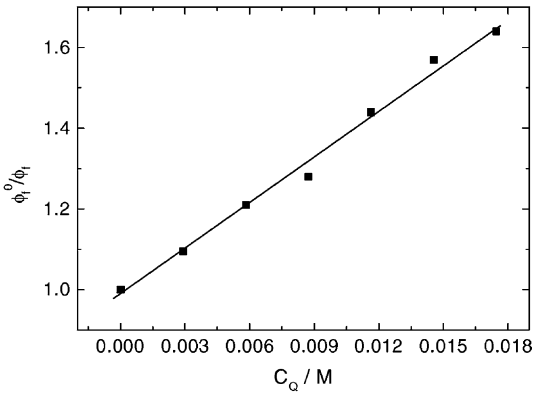

Fig. 4. Plots of relative reciprocal quantum yield of fluorescence ϕ_f^0/ϕ_f versus concentration C_Q of 9,10-diphenylanthracene. The line is drawn for a Stern–Volmer constant $K_{SV} = 37\,M^{-1}$.

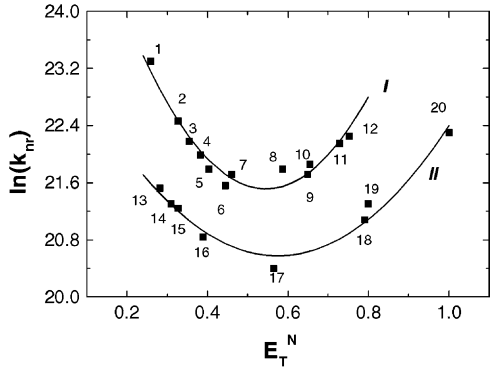

Fig. 5. Plots of logarithm of the rate constant k_{nr} of radiationless decay at 25 °C vs. the solvent polarity parameter E_T^N for 20 solvents. The number codes of the solvents are given in Table 1. The solid curves are the best fits.

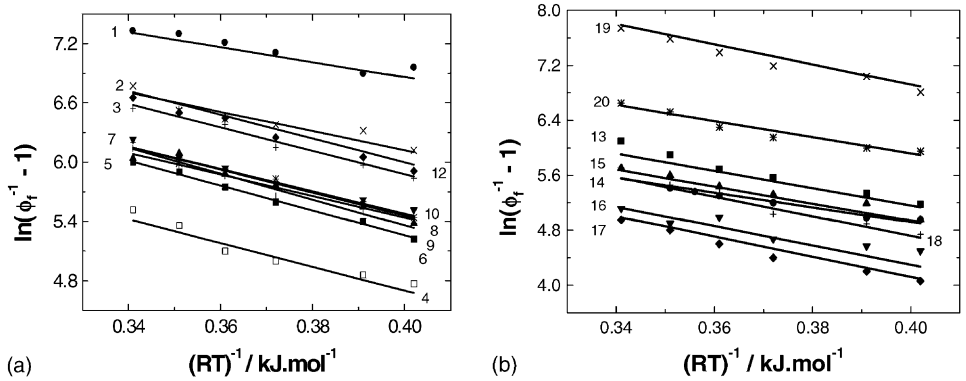

Fig. 6. Plots of the logarithm of the rate constant k_{nr} of radiationless decay vs. the reciprocal of temperature $1/RT$ for group I solvents (a) and for group II solvents (b). The number codes of the solvents are given in Table 1. The Arrehnius energies E_V and the preexponential factors A_0 as obtained from the straight lines are given in Table 1.

center ($E_{T0}^N = 0.54$) (±0.006) for group I and 0.58 (±0.01) for group II, respectively.

$$\ln(k_{nr}) = \ln(k_{nr}^0) + B[E_T^N - (E_{T0}^N)]^2 \quad (8)$$

We can also see from Fig. 5 that the division of the solvents differs very much from that in the plots of the solvatochromic shifts against E_T^N. This fact indicates that there is another important factor besides the solvent polarity to influence the process from the E^* to I^* states.

4.6. Arrhenius energies

We have measured the quantum yields of fluorescence in 19 solvents except formic acid (because other reactions are observed for compound **1** in formic acid, so the solvent is omitted) as a function of temperature from 25 to 80 °C if possible. The data are shown in Fig. 6. They are described by Eq. (9), the Arrhenius intercept A_0 and the Arrhenius energy E_V are also listed in Table 1. Fig. 6a shows plots of the logarithm of k_{nr} at different temperatures against the reciprocal of RT in group I solvents, and Fig. 6b shows that in group II solvents, here R is the gas constant.

$$\ln k_{nr} = \ln[k_f^{AV}(\phi_f^{-1} - 1)] = \ln A_0 - \frac{E_V}{RT} \quad (9)$$

From Table 1, we can see that the Arrhenius energies E_V exhibit a strong solvent dependence, while the Arrhenius intercept A_0 shows a very slight dependence on solvent polarity. The average of $\ln A_0$ is 26.6. A plot of the values of E_V versus E_T^N shown in Fig. 7 shows a similar nonlinear relation and division to those in Fig. 5. The difference to the relation shown in Fig. 5 is that a maximum, not a minimum, at a certain polarity is observed for each group. Best fits the data in Fig. 7 using Eq. (10) yield an intercept $E_V^0 =$ 13.1 (±0.3) kJ/mol for group I and 15.1 (±0.8) kJ/mol for group II, with an amplitude $\beta = -50.9$ (±10.9) kJ/mol for group I and −27.5 (±8.6) kJ/mol for group II and a center ($E_{T0}^N)' = 0.57$ (±0.02) for group I and 0.65 (±0.02) for group II.

$$E_V = E_V^0 + \beta[E_T^N - (E_{T0}^N)']^2 \quad (10)$$

Note that two the values of β/RT (20.5 and 11.1 at $T =$ 298 K) are very close to the corresponding values of B from Eq. (8) within the experimental errors, while that of $(E_{T0}^N)'$ are relatively larger than E_{T0}^N.

4.7. The rate constant of internal conversion decay

As discussed in Section 1, the decay reaction for stilbazolium dyes fits the extreme case $k_{IC} \gg k_2$. But for compound **1**, we assume that the decay scheme coincides with another extreme case, e.g., $k_{IC} \ll k_2$, based on the following fact that a plot of the logarithms of k_{nr} against the solvent viscosity according to $k_{nr} = C(1/\eta)^x$ gives out $x = -0.28$ (with $C = 1.78\,ns^{-1}$, $R^2 = 0.52$, $N = 19$ except that in chloroform) (not shown). This value of x is close to that for rhodamine B ($x = -0.38$) [12], but very much smaller

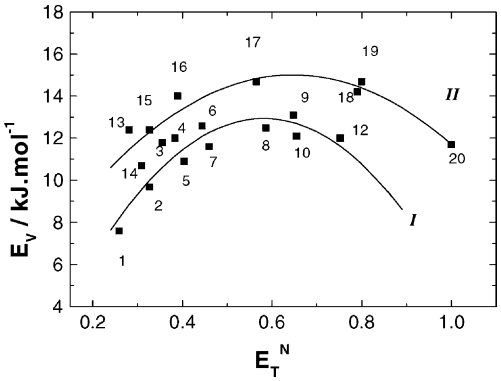

Fig. 7. Plots of the Arrhenius energies in groups I and II solvents in the region of 25–80 °C vs. E_T^N. The number codes of the solvents are given in Table 1. The solid curves are the best fits.

than that for common TICT compounds shown in [9] with $0.5 < x < 1$. Therefore, Eq. (1) can be converted to

$$k_I = \frac{k_{IC}k_1}{k_2} = k_{IC}K_{12} \tag{11}$$

Here, K_{12} is the equilibrium constant for interconversion between the E* and I* states. So the temperature dependence of k_I is determined by the temperature dependence of k_{IC} and K_{12}. In general, the temperature dependence of the internal conversion and intersystem crossing should not follow a simple Arrhenius type law, and the internal conversion probability mainly reveals an exponential dependence on the energy gap between the I* and I states and a weak dependence on temperature [12,35,36]. So, k_{IC} can be expressed in terms of the energy gap law.

$$k_{IC} = A_{IC}\exp(-\Delta E_{10}) \tag{12}$$

Here, A_{IC} is the preexponential factor. So the linear Arrhenius behavior of k_{nr} is mainly due to the temperature dependence of K_{12}:

$$K_{12} = A_{12}\exp\left(-\frac{\Delta G_{EI}}{RT}\right) \tag{13}$$

Here, A_{12} is the preexponential factor, ΔG_{EI} is Gibbs free energy difference of the E* and I* states. In this case, we have $E_V = \Delta G_{EI}$ and $E_V^0 = \Delta G_{EI}^0$, here ΔG_{EI}^0 represents the Gibbs free energy difference of the E* and I* states in the solvents with a polarity $(E_{T0}^N)'$. The positive value indicates that the I* state is higher than the E* state in free energy [12]. The polarity dependence of k_{nr} is the product of the polarity dependence of ΔE_{10} and ΔG_{EI}. Eq. (14) can be deduced using Eqs. (2) and (10)–(13) as follows. First, the ΔE_{10} in Eq. (12) is replaced by the right side of Eq. (2), and the ΔG_{EI} in Eq. (13) is also replaced by the right side of Eq. (10). Then, the resulted Eqs. (12) and (13) are taken into Eq. (11) to yield Eq. (14) by combining the common terms.

$$k_I = A\exp\left\{-\left(\frac{\beta}{RT}\right)[E_T^N - (1+g)(E_{T0}^N)']^2\right\} \tag{14}$$

Here, the preexponential factor $A = A_{IC}A_{12}\exp\{-\Delta E_{10}^0 - (\Delta G_{EI}^0)/RT + \beta g(g+2)(E_{T0}^N)'^2/RT\}$, $g = \kappa RT/[2\beta(E_{T0}^N)']$. Comparison of Eqs. (14) and (8) gives that $A = k_{nr}^0$, $-\beta/RT = B$, and $(1+g)(E_{T0}^N)' = E_{T0}^N$ under the condition of $k_{nr} \cong k_I$. The value of κ_1 can be calculated as $\kappa_1 = 1.2$ kJ/mol E_T^N based on the known values of $(E_{T0}^N)_1' = 0.57$, $(1+g_1)(E_{T0}^N)_1' = 0.54$, and $\beta_1 = -50.9$ for the solvent in group I, and $\kappa_2 = 1.6$ kJ/mol E_T^N according to $(E_{T0}^N)_2' = 0.65$, $(1+g_2)(E_{T0}^N)_2' = 0.58$, and $\beta_2 = -27.5$ for the solvent in group II. We can see that the two κ-values are very close within the experimental errors, supporting that $k_{IC} \ll k_2$. Additionally, the dipole moment of the I state can be estimated as $\mu_g^I = 6.4$ D by taking both values of $\kappa = 0.5\ (\kappa_1 + \kappa_2) = 1.4\ (117\,\text{cm}^{-1})$ and $\mu_e^{I^*} = 4.6$ D (Table 3) into the relation $\kappa = 2(\mu_e^I - \mu_g^I)\mu_e/hca_w^3$. Both values of μ_g^I and μ_g are very close to each other. This also indicates the case of $k_{IC} \ll k_2$. The k_{nr} corrected for the solvent polarity, k_{corr}, can be given from Eq. (14) by the division of k_{nr} by term of $\exp\{B[E_T^N - (E_{T0}^N)]^2\}$.

$$\begin{aligned} k_{corr} &= k_{nr}\exp\left\{\left(\frac{\beta}{RT}\right)[E_T^N - (E_{T0}^N)]^2\right\} \\ &= A_{corr}\exp\left\{-\frac{\Delta G_{EI}^0 - \beta g(g+2)(E_{T0}^N)'^2}{RT}\right\} \end{aligned} \tag{15}$$

Here, A_{corr} is preexponential factor. Because the term $\beta g(g+2)(E_{T0}^N)'^2$ is very small, e.g., it is 1.75 kJ/mol for group I and 2.70 kJ/mol for group II, so the slope of the linear Arrhenius relation between the k_{corr} and $1/RT$ is mainly determined by ΔG_{EI}^0 according to Eq. (15). The resulted intercepts and slopes are listed in Table 1. We can also see from Table 1 that: (a) both of the intercepts and slopes do exhibit a very slight solvent polarity dependence and (b) the values of A_{corr} are very close to that of A_0, while the values of the slope ΔG_{EI}^0 are nearly equal to that of E_V^0 of Eq. (10) for groups I and II, respectively, within the experimental errors. Both of these also coincide with the extreme case of $k_{IC} \ll k_2$.

Otherwise, very difference is observed from comparisons of either the correlation or divisions in the plots of the solvatochromic shifts versus E_T^N with those in the plots of either ϕ_f or $\ln k_{nr}$, or E_V versus E_T^N. This fact indicates that there is another important factor besides solvent polarity, e.g., due to twist of molecule in excited state, to influence the process from E* to I* states. Note that the division of solvents in the linear relationship of ΔE_{10} with E_T^N is rationally assumed to be difference from that in the linear relationship of the solvatochromic shifts with E_T^N, but be similar to that in the nonlinear relationship of other photophysical properties such as ϕ_f or $\ln k_{nr}$, or E_V with E_T^N because of the occurrence of molecular twisting before molecules undergo the transition from the I* to I states.

5. Conclusions

The solvatochromic shifts of compound **1** show a linear relation with increasing E_T^N, in which all solvents are divided into two groups, one includes n- and π-type solvents, the other involves alkane chloride and HBD solvents. The dipole moment of the fluorescence emission and twisted intramolecular charge transfer states were estimated.

The logarithm of the rate constants of radiationless decay of compound **1** exhibit a solvent polarity modulation, but are independent on the solvent viscosity. The solvent polarity influences exhibit a nonlinear relation in which all solvents are also divided into two groups, but the division differs very much from that in the linear relation between solvatochromic shifts and E_T^N.

The reaction scheme of decay from the excited singlet state is controlled by the equilibrium constant for interconversion between the twisted and planar conformations.

Acknowledgements

Authors are thankful to Professor Bao-Wen Zhang of the Technology Institute of Physics and Chemistry, the Chinese Academy of Sciences for her kindly offering of the sample 4-nitro-4′-(*N*,*N*-dimethylamino)-stilbene. Authors also thank Yi Zhang, Yu Chen, and Zheng-Wang Qu for their kind help in the calculations and Junlin Yang for his kind analysis of spectra. This project is supported by NSCF (Nos. 29832030 and 29682001).

References

[1] H. Görner, H. Gruen, J. Photochem. 28 (1985) 329.
[2] D. Bringman, N.P. Ernsting, J. Chem. Phys. 102 (1995) 2691.
[3] H. Ephardt, P. Fromherz, J. Phys. Chem. 93 (1989) 7717.
[4] B. Strehmel, W. Rettig, J. Biomed. Opt. 1 (1996) 98.
[5] B. Strehmel, H. Seifert, W. Rettig, J. Phys. Chem. 101 (1997) 2232.
[6] P. Fromherz, K.H. Dambacher, H. Ephardt, A. Lambacher, C.O. Müller, R. Neigl, H. Schaden, O. Schenk, T. Vetter, Ber. Bunsenges. Phys. Chem. 95 (1991) 1333.
[7] L.M. Loew, S. Scully, L. Simpson, A.S. Waggoner, Nature 281 (1979) 497.
[8] Z.R. Grabowski, K. Rotkiewiez, A. Siemiarczuk, D.J. Cowley, W. Baumann, Nouv. J. Chim. 3 (1979) 443.
[9] W. Rettig, Angew. Chem. 98 (1986) 969; Angew. Chem., Int. Ed. Engl. 25 (1986) 971.
[10] J. Hicka, M. Vandersall, Z. Babarogic, K.B. Eisenthal, Chem. Phys. Lett. 116 (1985) 18.
[11] K.A. Zachariasse, M. Grobys, Th. Haar der van, A. Hebecker, Yu.V. I1'ichev, Y.-B. Jiang, O. Morawski, W. Kühnle, J. Photochem. Photobiol. 102 (1996) 59.
[12] K.G. Casey, E.L. Quitevis, J. Phys. Chem. 92 (1988) 6590.
[13] C. Reichardt, Solvents and Solvent Effects in Organic Chemistry, 2nd Edition, VCH, Weinheim, 1988.
[14] K. Dimroth, C. Reichardt, T. Siepmann, F. Bohlmann, Liebigs Ann. Chem. 727 (1969) 93.
[15] S.T. Abdel-Halim, M.H. Abdel-Kader, U.E. Steiner, J. Phys. Chem. 92 (1988) 4324.
[16] E. Akesson, V. Sundström, T. Gillbro, Chem. Phys. Lett. 121 (1985) 513.
[17] H. Görner, J. Photochem. Photobiol. A 40 (1987) 325.
[18] H. Gruen, H. Görner, J. Phys. Chem. 93 (1989) 7144.
[19] R. Lapouyade, A. Kuhn, J.-F. Letard, W. Rettig, Chem. Phys. Lett. 208 (1993) 48.
[20] M. Born, Z. Phys. 1 (1920) 45.
[21] T. Abe, J. Phys. Chem. 90 (1986) 713.
[22] H. Ephardt, P. Fromherz, J. Phys. Chem. 95 (1991) 6792.
[23] G.S. He, L.X. Yuan, P.N. Prasad, Opt. Commun. 140 (1997) 49.
[24] C.F. Zhao, G.S. He, J.D. Bhawalker, C.F. Park, P.N. Prasad, Chem. Mater. 7 (1995) 1979.
[25] C.L. Zhan, D.Y. Wang, Ganguang Kexue yu Guang Huaxue. 18 (2000) 121.
[26] J.A. Riddick, W.B. Bunger, T.K. Sakano, Organic Solvents, Physical Properties and Methods and Purification, Vol. 2, 4th Edition, Wiley, New York, 1986.
[27] T. Karstens, K. Kobs, J. Phys. Chem. 84 (1980) 1871.
[28] E. Fischer, J. Phys. Chem. 71 (1967) 3704.
[29] M.J.S. Dewar, E.G. Zoebisch, E.F. Healy, J.J.P. Stewart, J. Am. Chem. Soc. 107 (1985) 3902.
[30] L. Bilot, A. Kawski, Z. Naturforsch. A 17 (1962) 621.
[31] W. Liptay, Z. Naturforsch. A 20 (1965) 1441.
[32] J.-F. Letard, R. Lapouyade, W. Rettig, J. Am. Chem. Soc. 115 (1993) 2441.
[33] G. Liu, L. Heisler, L. Li, M.G. Steinmetz, J. Am. Chem. Soc. 118 (1996) 11412.
[34] H. Görner, D. Schulte-Frohlinde, J. Phys. Chem. 89 (1989) 4105.
[35] R. Englman, J. Jortner, Mol. Phys. 18 (1970) 145.
[36] J. Jortner, S.A. Rice, R.M. Hochstrasser, Adv. Photochem. 7 (1969) 149.